ORIGINAL ARTICLE

An Ultra-High Field Study of Cerebellar Pathology in Early Relapsing-Remitting Multiple Sclerosis Using MP2RAGE

Mário João Fartaria, MSc,*† Kieran O'Brien, PhD,‡§ Alexandra Şorega, MD,‖ Guillaume Bonnier, PhD,*¶ Alexis Roche, PhD,*†# Pavel Falkovskiy, PhD,*†# Gunnar Krueger, PhD,** Tobias Kober, PhD,*†# Meritxell Bach Cuadra, PhD,†#†† and Cristina Granziera, MD, PhD¶‡‡

Objectives: The aim of this study was to study focal cerebellar pathology in early stages of multiple sclerosis (MS) using ultra-high-field magnetization-prepared 2 inversion-contrast rapid gradient-echo (7T MP2RAGE).

Materials and Methods: Twenty early-stage relapsing-remitting MS patients underwent an MP2RAGE acquisition at 7 T magnetic resonance imaging (MRI) (images acquired at 2 different resolutions: $0.58 \times 0.58 \times 0.58$ mm^3, 7T_0.58, and $0.75 \times 0.75 \times 0.90$ mm^3, 7T_0.75) and 3 T MRI ($1.0 \times 1.0 \times 1.2$ mm^3, 3T_1.0). Total cerebellar lesion load and volume and mean cerebellar lesion volume were compared across images using a Wilcoxon signed-rank test. Mean T1 relaxation times in lesions and normal-appearing tissue as well as contrast-to-noise ratio (CNR) measurements were also compared using a Wilcoxon signed-rank test. A multivariate analysis was applied to assess the contribution of MRI metrics to clinical performance in MS patients.

Results: Both 7T_0.58 and 7T_0.75 MP2RAGE showed significantly higher lesion load compared with 3T_1.0 MP2RAGE ($P < 0.001$). Plaques that were judged as leukocortical in 7T_0.75 and 3T_1.0 MP2RAGEs were instead identified as WM lesions in 7T_0.58 MP2RAGE. Cortical lesion CNR was significantly higher in MP2RAGEs at 7 T than at 3 T. Total lesion load as well as total and mean lesion volume obtained at both 7 T and 3 T MP2RAGE significantly predicted attention ($P < 0.05$, adjusted $R^2 = 0.5$), verbal fluency ($P < 0.01$, adjusted $R^2 = 0.6$), and motor performance ($P = 0.01$, adjusted $R^2 = 0.7$).

Conclusions: This study demonstrates the value of 7 T MP2RAGE to study the cerebellum in early MS patients. 7T_0.58 MP2RAGE provides a more accurate anatomical description of white and gray matter pathology compared with 7T_0.75 and 3T_1.0 MP2RAGE, likely due to the improved spatial resolution, lower partial volume effects, and higher CNR.

Cerebellum damage is common in multiple sclerosis (MS) at all disease stages.[1] However, while cerebellar atrophy and focal white matter (WM) lesions have been reported in both relapsing-remitting[2,3] and progressive MS[4–6] patients, there are only a few reports on focal pathology in the cerebellar cortical layers.[2,7,8] The cerebellar cortex is approximately 3 to 5 times smaller than the cerebral cortex (~240 μm thickness),[9] which makes it difficult to study with conventional magnetic resonance imaging (MRI) techniques.[1,10] Intracortical MS lesions in the cerebellum are often very small and therefore suspect to large partial volume effects in routine clinical imaging protocols. Moreover, demyelinating lesions in cerebellar cortical gray matter (GM) have poorer contrast than cortical lesions in the brain hemispheres due to the generally lower myelin content in the cerebellar cortex.[1,10] Ultra–high-field MRI (7 T) has been shown to be a valuable tool to assess the contribution of cortical pathology in the brain hemispheres to clinical disability.[11–13] Still, the question remains whether the higher resolutions enabled by 7 T MRI improve the detection of MS cerebellar pathology compared with clinical field strengths and how this correlates to the patient's symptoms.

Ultra–high-field magnetization-prepared 2 inversion-contrast rapid gradient-echo (MP2RAGE) may have high clinical value by potentially improving the study of focal cerebellar pathology in early stages of MS. It has been previously shown that for hemispheric cortical lesion detection at 3 T, MP2RAGE is nearly as sensitive as double inversion recovery, which is considered the criterion standard for lesion detection in the cortical layers[14,15]; 3 T MP2RAGE is also more sensitive than 3D fluid-attenuated inversion recovery for WM lesion (WML) detection.[14,15] In addition, MP2RAGE can provide T1 relaxometry measurements that have been shown to be directly related to properties of the brain tissue in both physiological[16] and pathological conditions (ie, inflammation and degeneration).[17–19] MP2RAGE images radically reduce spatial signal intensity inhomogeneities stemming from physical effects related to the excitation and reception of the MR signal,[20,21] which is a significant asset at 7 T. Finally, further practical limitations of MP2RAGE at ultra–high-field have been removed by adding high permittivity dielectric pads and inversion pulses with optimized efficiency in difficult regions like the temporal lobe or the cerebellum.[21] Consequently, we hypothesize that ultra–high-field MP2RAGE[11,22] should benefit and improve the detection and characterization of focal cerebellar pathology in MS patients. In addition, we expect that 7 T MP2RAGE will help to ameliorate the clinicoradiological correlations of cerebellar focal pathology.

In this work, we compared cerebellar manual lesion count, volume, and T1 relaxometry values as obtained in 7 T and 3 T MP2RAGE images. Also, we assessed the relationship between cerebellar lesion characteristics at different resolution and magnetic field-strength, and patient clinical scores.

MATERIALS AND METHODS

Subjects and MRI Acquisition

Twenty patients (15 women, 5 men), diagnosed with relapsing remitting MS (RRMS) according to the revised McDonald criteria,[23]

were imaged on a 7 T MRI research scanner (Siemens Healthcare, Germany) and a 3 T MRI scanner (MAGNETOM Trio, A Tim System; Siemens Healthcare, Germany) using 32-channel head coils (Nova Medical at 7 T and Siemens Healthcare at 3 T). Inclusion criteria were stable disease on high-dosage interferon beta or fingolimod, less than 6 years' disease duration, and no other concomitant neurological or psychiatric disease. The imaging was performed between January 2012 and November 2013, and the median time between successive MR examinations at 3 T and 7 T was 9 months (range, 2–14 months). Due to the order of acquisitions performed in the course of the study (first time point 3 T → 7 T → second time point 3 T), the second 3 T scan session acquired 2 years after the first 3 T session (21.4 ± 2.5 months; range, 16–27 months) could be used to assess whether the cerebellar lesion load was stable over time. The study was approved by the ethics committee of our institution, and all subjects gave written informed consent before participation.

Whole-brain 3D MP2RAGE images were acquired at 3 T using a clinical resolution of $1.0 \times 1.0 \times 1.2$ mm^3 (3T_1.0) and at 7 T using a high resolution of $0.75 \times 0.75 \times 0.9$ mm^3 (7T_0.75). In addition, 2 separate MP2RAGE images of $0.58 \times 0.58 \times 0.58$ mm^3 (7T_0.58) were acquired at 7 T targeting the cerebellum. The 2 acquisitions were performed separately to mitigate motion corruption. The two 7T_0.58 MP2RAGE images were first spatially normalized using rigid registration, performed by the ELASTIX C++ library[24] and then averaged to improve the signal-to-noise ratio (SNR). The acquisition parameters for each protocol are detailed in Table 1. At 7 T, 3 dielectric MR-invisible pads were placed under the subject's neck just below the ears. These pads were used to improve the inversion pulse efficiency over the cerebellum.[21] The acquisition protocols were designed to study cerebellar pathology in MS and had the goal to reach the highest resolution possible without penalizing the SNR and contrast-to-noise ratio (CNR), while maintaining clinically acceptable scan times. Both 7 T protocols were optimized in this respect as reported in O'Brien et al.[21] The 3 T protocol follows the recommendations given in the original MP2RAGE[20] publication with the aim of optimizing GM/WM contrast.
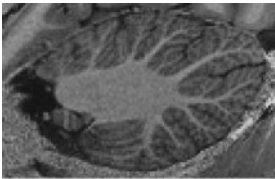
Manual Segmentation

Cerebellar lesions were identified and delineated by consensus between 1 radiologist (A.S.) and 1 neurologist (C.G.), with 3 and 11 years of experience, respectively. The observers were blinded to the clinical status of the patients and aware of the potential artifacts and pitfalls of MS reading in MRI.[14,25,26] Subsequently, each lesion was labeled as either pure focal WML or a focal GM lesion. The latter was further categorized into 1 of the 2 cerebellar GM lesion classes[1,7]: (1) leukocortical, extensions of WML in the folia, affecting adjacent cortical tissue; (2) intracortical, lesions within the cerebellar cortex that do not reach the subcortical WM.

Total cerebellar lesion load (TcLL), total cerebellar lesion volume (TcLV), and the mean cerebellar lesion volume (McLV, volume of all lesions divided by the number of lesions) for all lesions and per each type of lesion were calculated. Mean T1 relaxation times were computed for lesions and for normal-appearing tissue in GM and WM, respectively. Mean T1 values for lesions were obtained by applying the lesion mask to the T1 maps obtained from the MP2RAGE scans. T1 values for the normal-appearing brain tissues were obtained by manually placing cubic-shaped regions of interest (ROI) with a volume of approximately 33 μL in every patient: 5 ROIs in the WM, 5 ROIs in the GM. Gray matter ROIs were selected to have similar standard deviations in T1 values from ROIs in the WM. To study the mixed WM/GM, 50% of the voxels from WM ROIs and 50% from GM ROIs were used to estimate mean T1 values.

The CNR in the 20 patients was estimated according to Equation 1, where m_{lesion} and m_{NA} are medians of signals from lesions and ROIs of normal-appearing WM or GM tissue, respectively, and σ^2_{lesion} and σ^2_{NA} represent the variances of signal intensities within lesions

TABLE 1. MRI Protocol

	7T_0.58 MP2RAGE	7T_0.75 MP2RAGE	3T_1.0 MP2RAGE
Resolution, mm^3	$0.58 \times 0.58 \times 0.58$	$0.75 \times 0.75 \times 0.9$	$1.0 \times 1.0 \times 1.2$
Matrix size	240×384	300×320	240×256
Slice/partitions	128	160	176
Orientation/readout	Slab selective axial/A → P	Nonselective sagittal/S → P	
Acquisition time	2×10 min 27 s	9 min 33 s	8 min 22 s
Acceleration factor	2	3	3
TR, ms	6000	6000	5000
TE, ms	3.49	2.92	2.89
TI, ms	800/2700	750/2350	700/2500
Flip angles,* degrees	4/5	4/5	4/5
Bandwidth, Hz/pixel	241	240	240
Target	Cerebellum	Whole brain	Whole brain

All the acquisitions are 3D.

*Flip angles for first/second GRE readout.

MRI indicates magnetic resonance imaging; MP2RAGE, magnetization-prepared 2 inversion-contrast rapid gradient-echo; TR, repetition time; TE, echo time; TI, inversion time.

and normal-appearing tissue from MP2RAGE images, respectively.[27] The variance was estimated using the median absolute deviation to mitigate partial volume effects.

$$CNR = \frac{(m_{lesion} - m_{NA})}{(\sigma^2_{lesion} + \sigma^2_{NA})}^2 \quad (1)$$

Clinical Assessment

Each subject underwent a neurological examination including the following cognitive and behavioral tests: (1) Brief Repeatable Battery of Neuropsychological Tests[28] (BRB-N), which examine verbal and spatial memory, sustained attention, information processing speed, and verbal fluency on semantic cues; (2) the Hospital Anxiety and Depression scale[29] (HAD); (3) the Fatigue Scale for Motor and Cognitive functions[30] (FSMC), which quantifies depressive mood symptoms and fatigue. The Expanded Disability Status Scale (EDSS)[31] and the Multiple Sclerosis Functional Composite (MSFC) scores were assessed by a certified neurologist (C.G.) to quantify motor performance.

Statistical Analyses

All statistical analyses were performed using the R software version 3.2.2. Lesion count and volume in the 3 different images were compared using a paired Wilcoxon signed-rank tests. The same statistical test was used to compare mean T1 relaxation times between lesions and normal-appearing tissue. Contrast-to-noise ratio between lesional and normal-appearing tissue in the 3 different images were compared using a paired Wilcoxon signed-rank test. For each clinical score, a correlation analysis was performed using a general linear model with TcLL, TcLV, and McLV (for all types of lesions) as regressors and the clinical score as the predicted outcome. Age, sex, education years, anxiety, and depression scores (HAD) were considered as covariates because they may affect patients' cognitive performance.[32,33] Backward stepwise analyses were performed to select the best prediction model for each clinical score. Bonferroni correction was applied for multiple comparisons. The significant variables were identified with a *P* value of < 0.05.

RESULTS

Clinical Scores

The mean patient age at the time of the first examination was 34.9 years (range, 21–46 years); 15 women, with a mean age of 36.5 years (range, 24–46 years), and 5 men, with a mean age of 30.0 years (range, 21–40 years). The mean disease duration (duration since the first symptoms and date of MRI examination) was less than 6 years (36.5 ± 21.8 months; range, 2–70 months). The median EDSS[31] was 1.5 (range, 1.0–2.0). Motor and cognitive scores are presented in Table 2. All patients were under immunomodulatory treatment (fingolimod or high-dosage interferon beta) before enrollment, and treatment did not change between scans.

Lesion Characteristics Comparison Among 7T_0.58, 7T_0.75, and 3T_1.0 MP2RAGEs

Except for 2 patients, no cerebellar lesion progression was observed between the first and second 3 T session. Notably, the 7 T scan was performed between the two 3 T time points. The 2 patients showed 2 new lesions each at the second 3 T time point; it was retrospectively confirmed by the experts that these lesions were not present in the 7 T images. We conclude that additional lesions picked up at 7 T are due to improved lesion conspicuity.

Figure 1A shows the number of lesions and their volume as obtained by manual segmentation using 7T_0.58, 7T_0.75, and 3T_1.0

TABLE 2. Clinical Scores in Our Cohort of Patients

| Clinical Test		Average ± STD
BRB-N	SRT-LTS	63.6 ± 7.1
	SRT-CLTR	60.4 ± 8.3
	SRT-D	11.5 ± 1.0
	SPART 10/36	24.3 ± 3.9
	SDMT	58.7 ± 7.8
	PASAT	49.3 ± 8.0
	WLG	30.2 ± 4.7
Motor performance	Leg function	−0.28 ± 1.12
	Arm function	−0.39 ± 0.85
HAD	Anxiety	7.5 ± 4.6
	Depression	3.4 ± 2.7
EDSS		1.6 ± 0.2

BRB-N indicates Brief Repeatable Battery of Neuropsychological Tests; SRT-LTS, Selective reminding test–long-term storage; SRT-CLTR, selective reminding test–consistent long-term retrieval; SRT-D, selective reminding test–delayed recall; SPART 10/36, spatial recall test; SDMT, symbol digit modalities test; PASAT, paced auditory serial addition test at 3s; WLG, word list generation HAD, hospital anxiety and depression; EDSS, expanded disability status scale.

MP2RAGE. Cerebellar lesion count was higher when performed on 7T_0.58 MP2RAGE compared with 7T_0.75 at 7 T and the 3T_1.0 MP2RAGE (*P* < 0.01), and on 7T_0.75 MPRAGE compared with 3T_1.0 MP2RAGE (*P* = 0.0015). No differences were observed for cerebellar lesion volume among the different images (*P* > 0.1403; 7T_0.58 MP2RAGE TcLV average: 268.3 μL; 7T_0.75 MP2RAGE: 304 μL; and 3T_1.0 MP2RAGE: 292 μL), which is further supported by the high correlation coefficients (ρ ≈ 1) between the manual segmentations obtained from the different protocols shown in Figure 1C. Figure 1B shows the size distribution of missed and detected lesions in 7T_0.75 and 3T_1.0 with respect to the high-resolution 7T_0.58 protocol. It can be seen that most of the missed lesions are small; notably, 70% of the missed lesions are smaller than 5 μL.

Examples of different cerebellar lesion types are presented in Figure 2. Count and volumes per lesion type are presented in Table 3. We can observe that all patients showed cerebellar WML and that the majority of cerebellar cortical lesions consisted of leukocortical lesions. Intracortical lesions were smaller and only observed in 2 patients using 7T_0.58 MP2RAGE and in one of those patients on 7T_0.75 MP2RAGE and 3T_1.0 MP2RAGE. Notably, 8 (13%) of 61 lesions classified as pure WMLs using 7T_0.58 MP2RAGEs were wrongly classified as leukocortical in the images with lower spatial resolution (see Fig. 3).

In 7T_0.58 images, 10% of total lesions were located within the cerebellar folia (see an exemplary set of missed lesions in Fig. 4). Only 36% of these lesions were detected using both 7T_0.75 images and 3T_1.0 MP2RAGE images.

Mean T1 relaxation times for lesion and normal-appearing tissue for the cerebellum at 7T_0.58, 7T_0.75, and 3T_1.0 MP2RAGE are shown in Figure 5. Except for intracortical lesions, T1 values in lesion tissue were longer than those in normal-appearing tissue (WM, *P* < 0.0001, and mixed WM/GM, *P* < 0.005). T1 values of intracortical lesions were not significantly different from normal-appearing GM, probably due to the small number of lesions observed in the whole cohort. There were no significant differences of CNR between lesion and normal-appearing WM between the 3 types of images (*P* > 0.07). However, the CNR between normal-appearing GM and lesions is significantly higher in the images acquired at higher field strength (*P* < 0.01, Fig. 6).
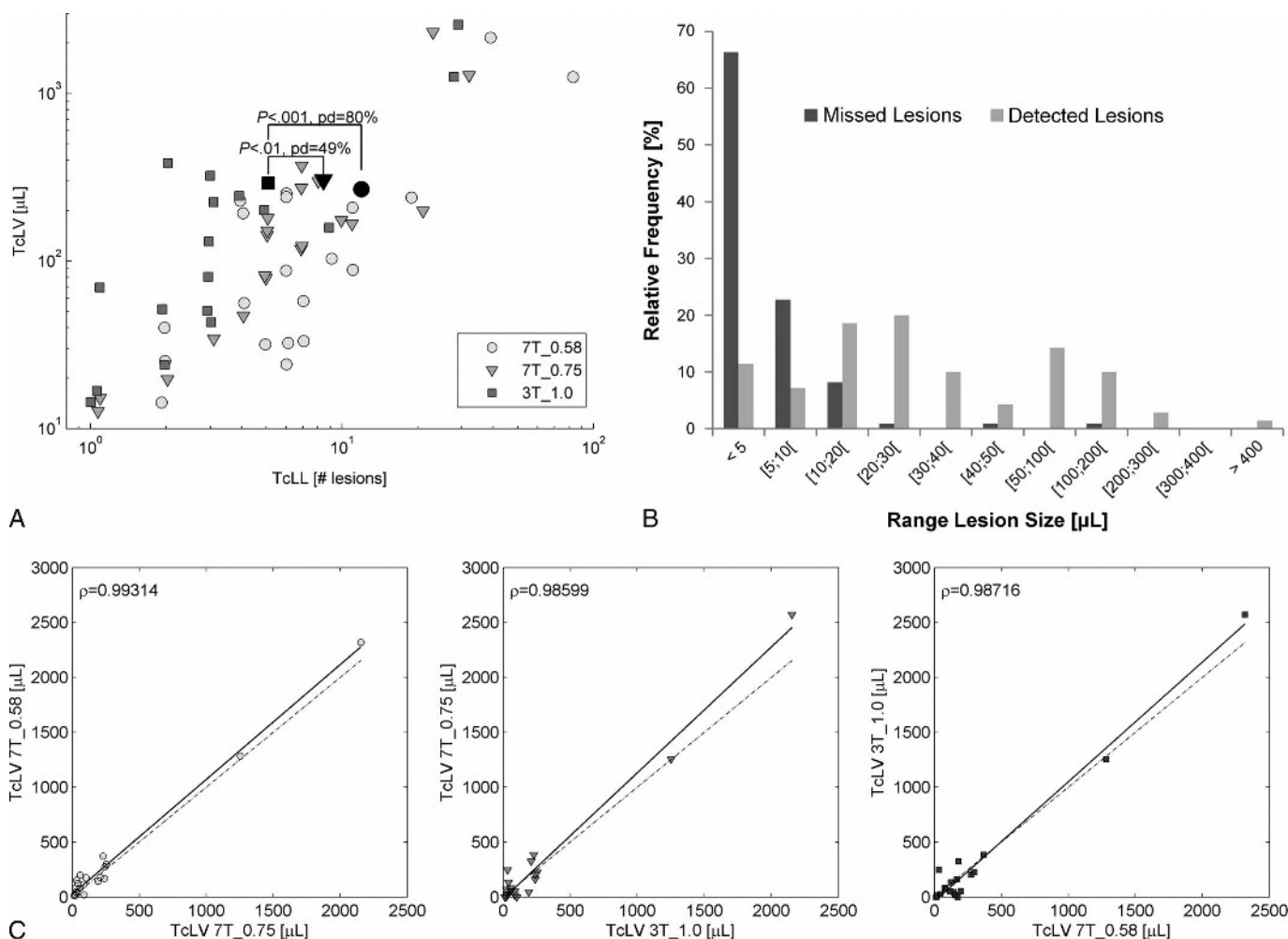
FIGURE 1. A, Log-log plot of manual segmentation results in terms of total lesion volume (TcLV, μL) and total lesion load (TcLL, number of lesions) obtained from 7T_0.58 (resolution, 0.58 × 0.58 × 0.58 mm³, circle), 7T_0.75 (resolution, 0.75 × 0.75 × 0.9 mm³, triangle), and 3T_1.0 (resolution, 1.0 × 1.0 × 1.2 mm³, square) images. Gray and black symbols represent the values per patient and average values, respectively. Percentage difference (pd) is shown for TcLL average between groups. B, Size distribution of missed (dark gray) lesions by 7T_0.75, and 3T_1.0, and detected (light gray) lesions by all protocols. C, Total cerebellar lesion volume (TcLV) correlation between 7T_0.58, 7T_0.75, and 3T_1.0 protocols and the respective Pearson correlation coefficient (ρ). The dash line represents the identity line, and the solid black line represents the best linear fit to the points.

Multiple Regression Analysis

General linear model using backward stepwise regression revealed significant ($P < 0.01$) association between cerebellar lesion characteristics and motor scores (see Table 4).

Leg function was correlated to (1) cerebellar McLV at 7T_0.58 MP2RAGE, HAD scores, and education (adjusted R^2, 0.7; corrected $P = 0.004$) and (2) cerebellar TcLL and TcLV at 7T_0.75 MP2RAGE combined with HAD scores and education (adjusted R^2, 0.7; corrected $P = 0.013$). None of the 3T_1.0 MP2RAGE scores appeared to be an independent predictor of leg function score.

Arm function was correlated to (1) cerebellar TcLL, TcLV, and McLV at 7T_0.58 MP2RAGE combined with age, education, and HAD scores (adjusted R^2, 0.7; corrected $P = 0.0006$) and (2) cerebellar TcLL, TcLV, and McLV at 3T_1.0 MP2RAGE combined with age, education, and HAD scores (adjusted R^2, 0.8; corrected $P = 0.0006$).

Both 7 T and 3 T cerebellar lesion characteristics correlated with cognitive scores (see Table 4). Cerebellar McLV at 7T_0.58 MP2RAGE together with sex, age, and HAD score correlated with the Selective reminding test-delayed score (adjusted R^2, 0.5; corrected $P = 0.03$). Cerebellar McLV at 3T_1.0 MP2RAGE, combined with age

and HAD score, was associated to the word list generation score (adjusted R^2, 0.6; corrected $P = 0.009$).

DISCUSSION

In this work, we assessed the performance of 7 T MP2RAGE to detect and segment intracortical, leukocortical, and subcortical focal cerebellar pathology in early-stage RRMS patients.

The study of focal pathology in the cerebellum is challenging due to its convoluted structure, characterized by intermingled WM and GM digitations in the folia and vermis.[34] MP2RAGE is a recently developed MRI sequence,[20] which provides a high WM-GM contrast at submillimeter spatial resolution at 7 T. In addition, adapted MP2RAGE protocols[21,35] have been shown to provide high SNR and low B1 bias in the cerebellum, even at very high spatial resolution. In this work, we compared 7T_0.58 MP2RAGE at 7 T using a 0.6-mm isotropic spatial resolution, with 7T_0.75 MP2RAGE at 7 T using slightly larger, but still submillimeter voxel size (0.75 mm in-plane and 0.9 mm slice thickness) and with 3T_1.0 MPRAGE acquired with 1 mm (almost) isotropic voxel size as in Kober et al[14] and Fartaria et al.[15] The protocols were optimized for optimal SNR and CNR at the given fields
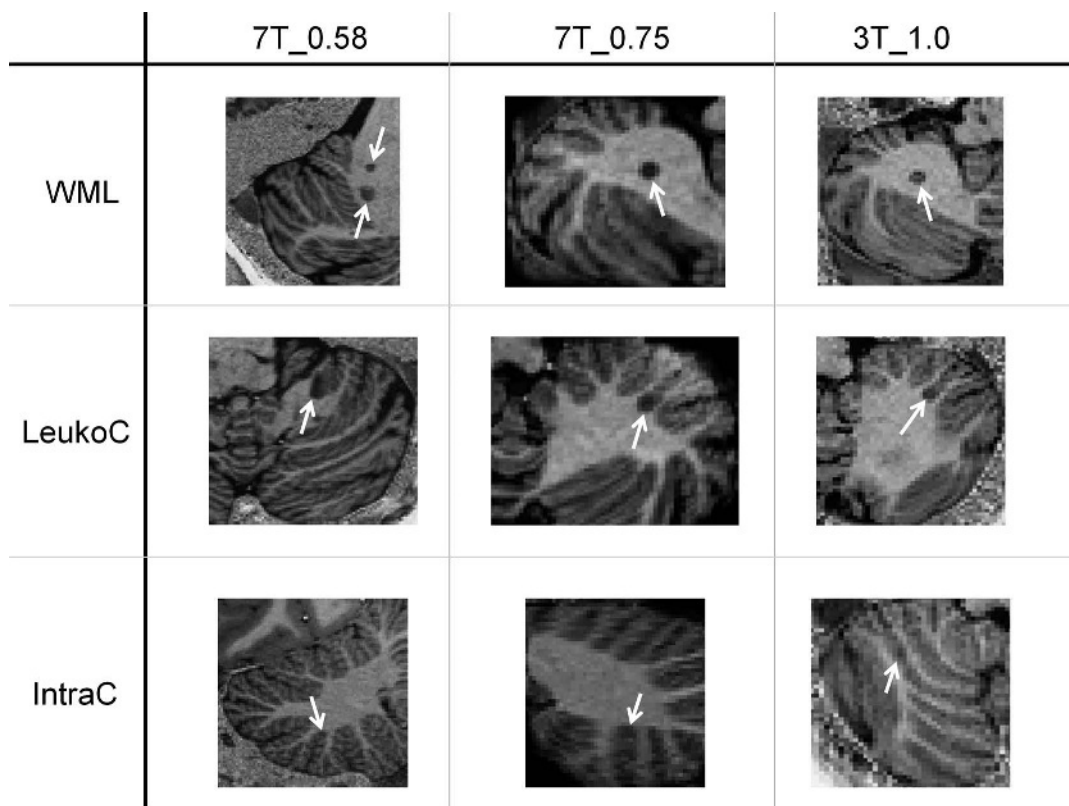
FIGURE 2. MP2RAGE patches of 7T_0.58 (resolution, 0.58 × 0.58 × 0.58 mm^3), 7T_0.75 (resolution, 0.75 × 0.75 × 0.9 mm^3), and 3T_1.0 (resolution, 1.0 × 1.0 × 1.2 mm^3), showing the 3 types of cerebellar lesions from different patients: white-matter lesions (WML), leukocortical lesion (LeukoC), and intracortical lesion (IntraC).

strengths and resolutions. For comparison, estimating the achievable SNR on a clinical 3 T scanner in the same acquisition time as the longest 7 T protocol (ie, 7T_0.58), an isotropic resolution of about 0.85 mm, could probably be reached.

Ultra-high-field MP2RAGE provided high sensitivity to lesion detection and detailed anatomical localization in the cerebellum. In fact, MP2RAGE at 7 T MRI allowed the detection of significantly higher lesion load than MP2RAGE at 3 T, likely due to the improved spatial resolution, lower-partial volume effects, and improved CNR for cortical lesions. In addition, lesion count in images with superior resolution at

7 T (7T_0.58) was significantly higher than the one obtained with slightly lower spatial resolution (7T_0.75) at the same magnetic field. Importantly, 7T_0.58 MP2RAGE permitted to anatomically localize 13% WMLs that were wrongly classified as leukocortical in the other 2 MP2RAGE acquisitions.

Our findings are in line with a previous histopathological study showing extensive focal cerebellar WM demyelination,[6,36,37] and they extend previous findings by providing new proof of important focal demyelination affecting the cerebellar cortex in vivo in early-stage MS patients with minimal impairment on stable therapy. A few previous works

TABLE 3. Number and Volume of Types of Lesions in Our Cohort of Patients

	7T_0.58				7T_0.75				3T_1.0			
	Median	**Min**	**Max**	**Total**	**Median**	**Min**	**Max**	**Total**	**Median**	**Min**	**Max**	**Total**
Lesion count (no.)												
WML	6	1	61	208	6	1	22	154	2	0	26	85
LeukoC	0	0	22	29	0	0	10	14	0	0	9	16
IntraC	0	0	1	2	0	0	1	1	0	0	1	1
Lesion volume, μL												
WML	81.7	14.3	1818.4	4527.0	136.9	12.7	2023.0	5011.4	75.0	0.0	1963.2	4467.6
LeukoC	0.0	0.0	434.7	812.3	0.0	0.0	730.0	1069.2	0.0	0.0	607.2	1368.0
IntraC	0.0	0.0	17.3	27.4	0.0	0.0	11.6	11.6	0.0	0.0	4.8	4.8

7T_0.58 (resolution, 0.58 × 0.58 × 0.58 mm^3), 7T_0.75 (resolution, 0.75 × 0.75 × 0.9 mm^3), 3T_1.0 (resolution, 1.0 × 1.0 × 1.2 mm^3).

Median indicates median values; Max, maximum value; Min, minimum value; Total, total number of lesions; WML, white-matter lesions; LeukoC, leukocortical lesions; IntraC, intracortical lesions.
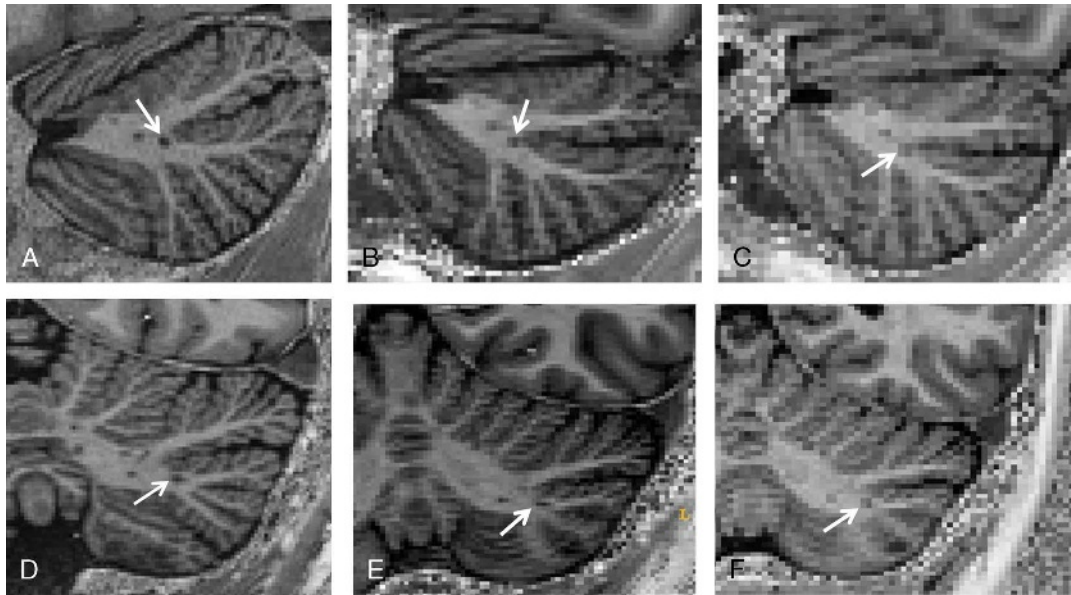
FIGURE 3. Example of misclassification of cerebellar WM lesions. A and D, Lesions classified as pure WM lesion using 7T_0.58 (resolution, 0.58 × 0.58 × 0.58 mm³). B and E, Lesions misclassified as leukocortical using 7T_0.75 (resolution, 0.75 × 0.75 × 0.9 mm³). C and F, Lesions misclassified as leukocortical using an image acquired at 3 T, 3T_1.0 (resolution, 1.0 × 1.0 × 1.2 mm³). Figure 3 can be viewed online in color at www.investigativeradiology.com.

used 2D double inversion recovery at 1.5 T and 3 T MRI as well as 2D fluid-attenuated inversion recovery at 3 T[38] to report focal cortical

lesions in the cerebellum at all MS stages including in clinical isolated syndrome,[2] RRMS,[2] and secondary progressive MS.[2] Yet, despite the
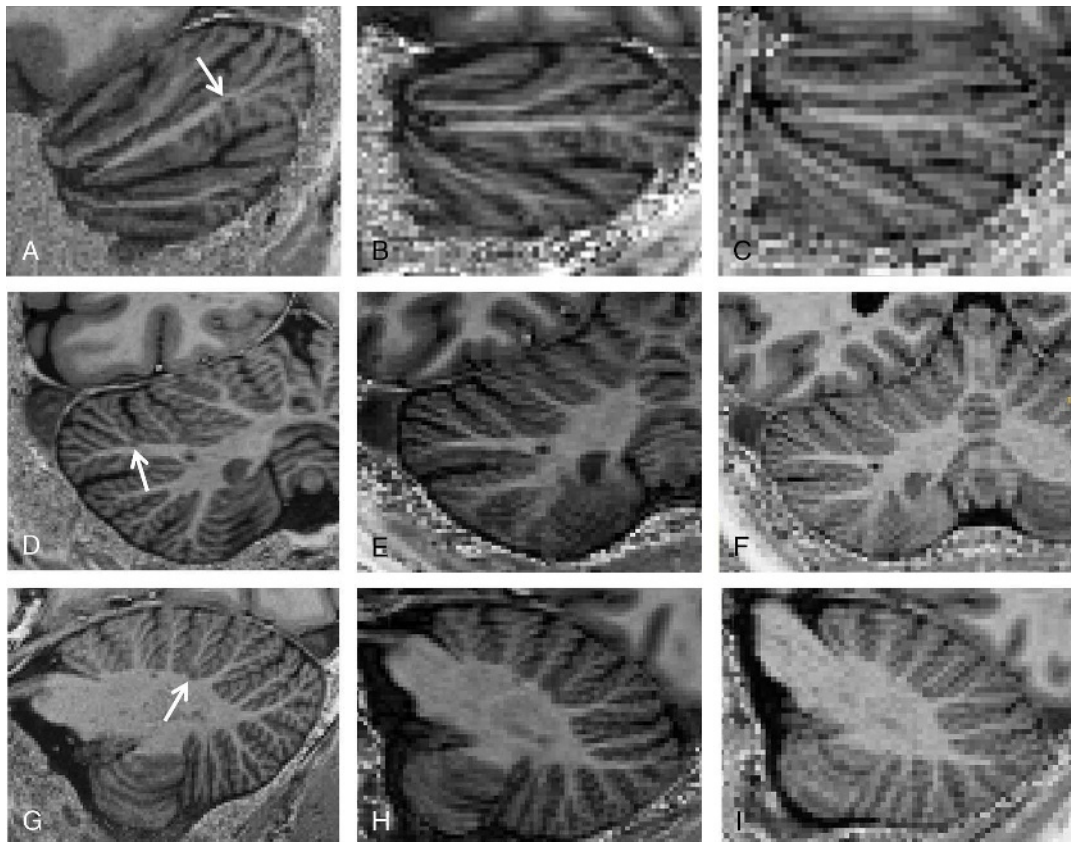
FIGURE 4. Example of lesions located within cerebellar folia: A, D, and G, Lesions detected using 7T_0.58 (resolution, 0.58 × 0.58 × 0.58 mm³). B, E, and H, Lesions missed using 7T_0.75 (resolution, 0.75 × 0.75 × 0.9 mm³). C, F, and I, lesions missed on image acquired at 3 T, 3T_1.0 (resolution, 1.0 × 1.0 × 1.2 mm³). Figure 4 can be viewed online in color at www.investigativeradiology.com.
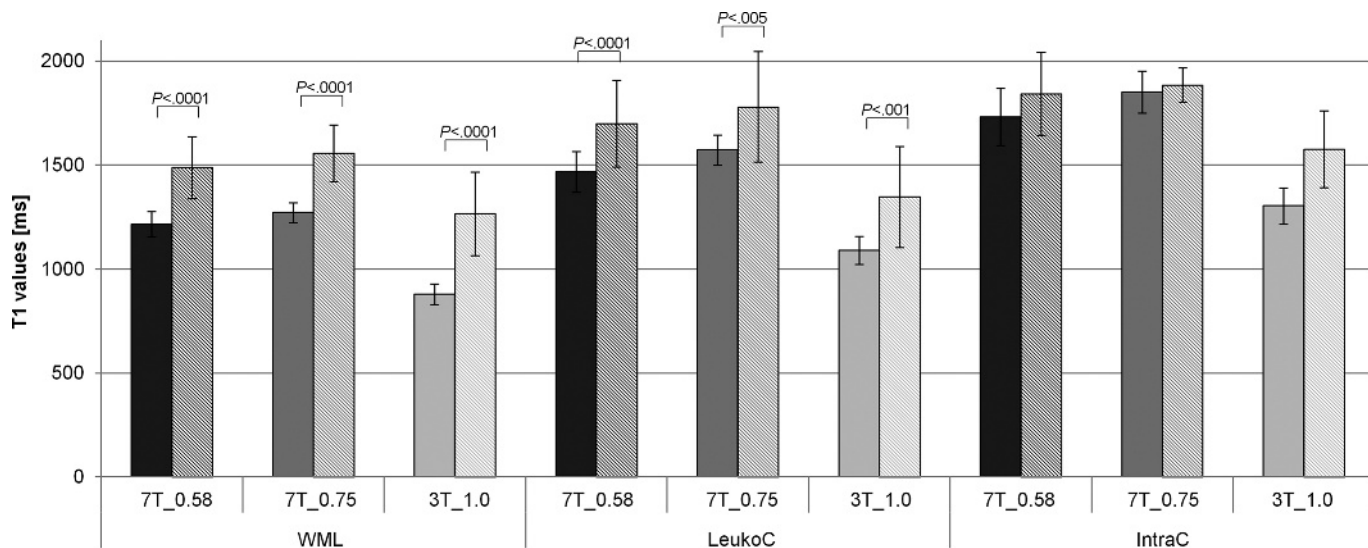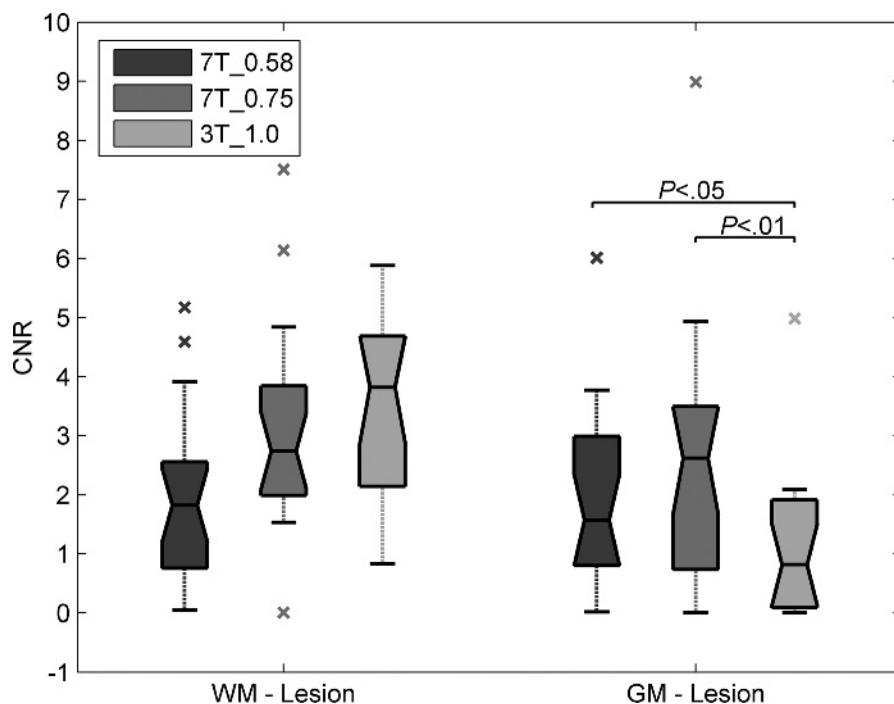
FIGURE 5. T1 relaxometry results using images acquired at 7T_0.58 (resolution, $0.58 \times 0.58 \times 0.58$ mm^3), 7T_0.75 (resolution, $0.75 \times 0.75 \times 0.9$ mm^3), and 3T_1.0 (resolution, $1.0 \times 1.0 \times 1.2$ mm^3). T1 values obtained in the cerebellum for normal-appearing WM, mixed WM/GM, and GM tissues (full bars) and WM (WML), leukocortical (LeukoC), and intracortical (IntraC) lesions (stripped bars). *P* values given are before Bonferroni correction.

valuable information acquired, all these studies suffered from low spatial resolution (slice thickness between 3 and 4 mm)[2,7] or poor GM-WM contrast.[38] Our work demonstrates the clear benefits of 7T_0.58 MP2RAGE to study in depth the presence and localization of cerebellar pathology compared with lower resolution protocols and lower field strength.

Interestingly, lesion count and volume as measured in 7T_0.58, 7T_0.75, and 3T_1.0 MP2RAGEs showed similar correlations with cognitive and motor performance in our cohort of MS patients. This was probably due to the fact that the best predictor of clinical scores was

lesion volume, which appeared to be equally estimated across MP2RAGEs. The remarkable absence of a significant difference in lesion volume between field strengths and different spatial resolutions is most probably due to missed lesions in the images with lower spatial resolution (ie, small lesions), as well as to the overestimation of lesion volumes at 3T_1.0 and 7T_0.75 MP2RAGE due to partial volume effects.

In addition to increased sensitivity, MP2RAGE provided microstructural characterization of focal cortical and subcortical pathology through T1 relaxometry maps. Pathological alterations in brain tissue, such as changes in myelination, gliosis, axonal injury, and loss as well

FIGURE 6. Box plots of CNR between lesions and normal-appearing WM (WM lesion), and lesions and normal-appearing GM (GM lesion) from all patients and from the 3 different types of images: 7T_0.58 (resolution, $0.58 \times 0.58 \times 0.58$ mm^3), 7T_0.75 (resolution, $0.75 \times 0.75 \times 0.9$ mm^3), and 3T_1.0 (resolution, $1.0 \times 1.0 \times 1.2$ mm^3). *P* values reported are after Bonferroni correction. The crosses in the plot represent outliers in our cohort.

TABLE 4. Multiple Regression Analyses Between MRI Scores

	7T_0.58		7T_0.75		3T_1.0	
	Corrected P	Adjusted R^2	Corrected P	Adjusted R^2	Corrected P	Adjusted R^2
SRT-LTS	0.42	0.32	1.69	0.15	0.75	0.12
SRT-CLTR	0.56	0.14	1.22	0.17	0.40	0.17
SRT-D	**0.03***	**0.53**	0.08	0.46	0.05	0.32
SPART 10/36	1.31	0.22	0.66	0.27	0.84	0.16
SDMT	0.54	0.33	0.14	0.42	0.06	0.49
PASAT	NS		NS		0.98	0.10
WLG	0.29	0.31	0.92	0.37	**0.009****	**0.56**
Leg Function	**0.004****	**0.69**	**0.013***	**0.67**	**0.002****	**0.68**
Arm Function	**0.0006*****	**0.69**	0.10	0.53	**0.0006*****	**0.80**
EDSS	0.36	0.34	0.98	0.23	0.43	0.32

Multiple regression analyses between MRI scores (performed at 7T_0.58, resolution, $0.58 \times 0.58 \times 0.58 \ mm^3$; 7T_0.75, resolution, $0.75 \times 0.75 \times 0.9 \ mm^3$; 3T_1.0 resolution, $1.0 \times 1.0 \times 1.2 \ mm^3$), covariates, and clinical scores (BRB-N, Brief Repeatable Battery of Neuropsychological Tests; MP, Motor Performance; and EDSS, Expanded Disability Status Scale). C. P values given are after Bonferroni correction. Difference in significance: ***high significance ($P < 0.001$), **middle significance ($P < .01$), *low significance ($P < .05$). NS, not significant, tests that did not reach significance before Bonferroni correction.

BRB-N: SRT-LTS indicates Selective reminding test–long-term storage; SRT-CLTR, selective reminding test–consistent long-term retrieval; SRT-D, Selective reminding test–delayed recall; SPART 10/36, spatial recall test; SDMT, Symbol digit modalities test; PASAT, Paced auditory serial addition test at 3s; WLG, word list generation. MP: Leg function; Arm function.

as edema and iron deposition influence T1 relaxation properties at different levels.[39] The sensitivity of T1 measurements at 7 T to contrast lesions compared with normal-appearing tissue was not influenced by spatial resolution and field strength, as similar differences were observed among 7T_0.58 to 7T_0.75 and 3T_1.0 T1 relaxometry maps.

A limitation of this study is the fact that we included a homogeneous cohort of early-stage RRMS patients under therapy, which prevented us to investigate focal cerebellar pathology at more advanced disease stages. Because of this, we also report a very limited number of purely intracortical lesions in our cohort. Considering the most recent guidelines,[40] future efforts should extend the current investigation to the entire MS spectrum.

In conclusion, ultra-high-field MP2RAGE provides an accurate description of cortical and subcortical cerebellar pathology, even in early-stage MS patients, due to the higher spatial resolution and CNR with less partial volume effects. Furthermore, in future, MP2RAGE T1 relaxometry may help to characterize in vivo the nature of cerebellar tissue pathology.

REFERENCES

1. Weier K, Banwell B, Cerasa A, et al. The role of the cerebellum in multiple sclerosis. *Cerebellum*. 2015;14:364–374.
2. Calabrese M, Mattisi I, Rinaldi F, et al. Magnetic resonance evidence of cerebellar cortical pathology in multiple sclerosis. *J Neurol Neurosurg Psychiatry*. 2010;81: 401–404.
3. Weier K, Penner IK, Magon S, et al. Cerebellar abnormalities contribute to disability including cognitive impairment in multiple sclerosis. *PLoS One*. 2014;9:e86916.
4. Howell OW, Schulz-Trieglaff EK, Carassiti D, et al. Extensive grey matter pathology in the cerebellum in multiple sclerosis is linked to inflammation in the subarachnoid space. *Neuropathol Appl Neurobiol*. 2015;41:798–813.
5. Gilmore CP, Donaldson I, Bö L, et al. Regional variations in the extent and pattern of grey matter demyelination in multiple sclerosis: a comparison between the cerebral cortex, cerebellar cortex, deep grey matter nuclei and the spinal cord. *J Neurol Neurosurg Psychiatry*. 2009;80:182–187.
6. Kutzelnigg A, Faber-Rod JC, Bauer J, et al. Widespread demyelination in the cerebellar cortex in multiple sclerosis. *Brain Pathol*. 2007;17:38–44.
7. Damasceno A, Damasceno BP, Cendes F. The clinical impact of cerebellar grey matter pathology in multiple sclerosis. *PLoS One*. 2014;9:e96193.
8. Geurts JJ, Calabrese M, Fisher E, et al. Measurement and clinical effect of grey matter pathology in multiple sclerosis. *Lancet Neurol*. 2012;11:1082–1092.
9. Marques JP, van der Zwaag W, Granziera C, et al. Cerebellar cortical layers: in vivo visualization with structural high-field-strength MR imaging. *Radiology*. 2010;254:942–948.
10. Timmann D, Konczak J, Ilg W, et al. Current advances in lesion-symptom mapping of the human cerebellum. *Neuroscience*. 2009;162:836–851.
11. Mainero C, Benner T, Radding A, et al. In vivo imaging of cortical pathology in multiple sclerosis using ultra-high field MRI. *Neurology*. 2009;73:941–948.
12. Saranathan M, Tourdias T, Kerr AB, et al. Optimization of magnetization-prepared 3-dimensional fluid attenuated inversion recovery imaging for lesion detection at 7 T. *Invest Radiol*. 2014;49:290.
13. Springer E, Dymerska B, Cardoso PL, et al. Comparison of routine brain imaging at 3 T and 7 T. *Invest Radiol*. 2016;51:469–482.
14. Kober T, Granziera C, Ribes D, et al. MP2RAGE multiple sclerosis magnetic resonance imaging at 3 T. *Invest Radiol*. 2012;47:346–52.
15. Fartaria MJ, Bonnier G, Roche A, et al. Automated detection of white matter and cortical lesions in early stages of multiple sclerosis. *J Magn Reson Imaging*. 2016; 43:1445–1454.
16. Deistung A, Schäfer A, Schweser F, et al. High-resolution MR imaging of the human brainstem in vivo at 7 Tesla. *Front Hum Neurosci*. 2013;7:710.
17. Bonnier G, Roche A, Romascano D, et al. Advanced MRI unravels the nature of tissue alterations in early multiple sclerosis. *Ann Clin Transl Neurol*. 2014;1:423–432.
18. Ganzetti M, Wenderoth N, Mantini D. Whole brain myelin mapping using T1- and T2-weighted MR imaging data. *Front Hum Neurosci*. 2014;8:671.
19. Bonnier G, Roche A, Romascano D, et al. Multicontrast MRI quantification of focal inflammation and degeneration in early multiple sclerosis. *Biomed Res Int*. 2015; 2015:569123.
20. Marques JP, Kober T, Krueger G, et al. MP2RAGE, a self bias-field corrected sequence for improved segmentation and T1-mapping at high field. *Neuroimage*. 2010;49:1271–1281.
21. O'Brien KR, Magill AW, Delacoste J, et al. Dielectric pads and low-B1+ adiabatic pulses: Complementary techniques to optimize structural T1w whole-brain MP2RAGE scans at 7 tesla. *J Magn Reson Imaging*. 2014;40:804–812.
22. Simioni S, Amarù F, Bonnier G, et al. MP2RAGE provides new clinically-compatible correlates of mild cognitive deficits in relapsing-remitting multiple sclerosis. *J Neurol*. 2014;261:1606–1613.
23. Polman CH, Reingold SC, Banwell B, et al. Diagnostic criteria for multiple sclerosis: 2010 revisions to the McDonald criteria. *Ann Neurol*. 2011;69: 292–302.
24. Klein S, Staring M, Murphy K, et al. Elastix: a toolbox for intensity-based medical image registration. *IEEE Trans Med Imaging*. 2010;29:196–205.
25. Geurts JJ, Bö L, Pouwels PJ, et al. Cortical lesions in multiple sclerosis: combined postmortem MR imaging and histopathology. *AJNR Am J Neuroradiol*. 2005;26:572–577.
26. Tallantyre EC, Morgan PS, Dixon JE, et al. 3 Tesla and 7 Tesla MRI of multiple sclerosis cortical lesions. *J Magn Reson Imaging*. 2010;32:971–977.

27. Falkovskiy P, Brenner D, Feiweier T, et al. Comparison of accelerated T1-weighted whole-brain structural-imaging protocols. *Neuroimage*. 2016;124:157–167.

28. Rao SM, Leo GJ, Bernardin L, et al. Cognitive dysfunction in multiple sclerosis. I. Frequency, patterns, and prediction. *Neurology*. 1991;41:685–691.

29. Zigmond AS, Snaith RP. The hospital anxiety and depression scale. *Acta Psychiatr Scand*. 1983;67:361–370.

30. Penner I, Raselli C, Stöcklin M, et al. The Fatigue Scale for Motor and Cognitive Functions (FSMC): validation of a new instrument to assess multiple sclerosis-related fatigue. *Mult Scler*. 2009;15:1509–1517.

31. Kurtzke JF. Rating neurologic impairment in multiple sclerosis an expanded disability status scale (EDSS). *Neurology*. 1983;33:1444–1452.

32. DeLuca J, Johnson SK, Beldowicz D, et al. Neuropsychological impairments in chronic fatigue syndrome, multiple sclerosis, and depression. *J Neurol Neurosurg Psychiatry*. 1995;58:38–43.

33. Phillips LJ, Stuifbergen AK. The relevance of depressive symptoms and social support to disability in women with multiple sclerosis or fibromyalgia. *Int J Rehabil Res*. 2010;33:142–150.

34. Stoodley CJ, Schmahmann JD. Evidence for topographic organization in the cerebellum of motor control versus cognitive and affective processing. *Cortex*. 2010;46:831–844.

35. O'Brien KR, Kober T, Hagmann P, et al. Robust T1-weighted structural brain imaging and morphometry at 7 T using MP2RAGE. *PLoS One*. 2014;9:e99676.

36. Lassmann H, Brück W, Lucchinetti CF. The immunopathology of multiple sclerosis: an overview. *Brain Pathol*. 2007;17:210–218.

37. Kutzelnigg A, Lucchinetti CF, Stadelmann C, et al. Cortical demyelination and diffuse white matter injury in multiple sclerosis. *Brain*. 2005;128:2705–2712.

38. Cerasa A, Passamonti L, Valentino P, et al. Cerebellar-parietal dysfunctions in multiple sclerosis patients with cerebellar signs. *Exp Neurol*. 2012;237:418–426.

39. Toga AW, Mazziotta JC. Brain mapping: An Encyclopedic Reference. In: Granziera C, Sprenger T. *Brain Inflammation, Degeneration, and Plasticity in Multiple Sclerosis*. London, UK: Academic Press; 2015;917–927.

40. Filippi M, Rocca MA, Ciccarelli O, et al. MRI criteria for the diagnosis of multiple sclerosis: MAGNIMS consensus guidelines. *Lancet Neurol*. 2016;15:292–303.